Proc. Natl. Acad. Sci. USA
Vol. 90, pp. 3068–3072, April 1993
Cell Biology

Ca^{2+} and Mn^{2+} influx through receptor-mediated activation of nonspecific cation channels in mast cells

(calcium stores/calcium release-activated calcium current/Fura-2/patch clamp)

CRISTINA FASOLATO*†, MARKUS HOTH*, GARY MATTHEWS‡, AND REINHOLD PENNER*

*Max-Planck-Institut für biophysikalische Chemie, Am Fassberg, 3400 Göttingen, Germany; and ‡Department of Neurobiology and Behavior, State University of New York, Stony Brook, NY 11794-5230

Communicated by Erwin Neher, December 18, 1992 (received for review November 23, 1992)

ABSTRACT **Whole-cell patch-clamp recordings of membrane currents and Fura-2 measurements of free intracellular calcium concentration ($[Ca^{2+}]_i$) were used to study calcium influx through receptor-activated cation channels in rat peritoneal mast cells. Cation channels were activated by the secretagogue compound 48/80, whereas a possible concomitant Ca^{2+} entry through pathways activated by depletion of calcium stores was blocked by dialyzing cells with heparin. Heparin effectively suppressed the transient Ca^{2+} release induced by 48/80 and abrogated inositol 1,4,5-trisphosphate-induced calcium influx without affecting activation of 50-pS cation channels. There was a clear correlation between changes in $[Ca^{2+}]_i$ and the activity of 50-pS channels. The changes in $[Ca^{2+}]_i$ increased with elevation of extracellular Ca^{2+}. At the same time, inward currents through 50-pS channels were diminished as more Ca^{2+} permeated. This effect was due to a decrease in slope conductance and a reduction in the open probability of the cation channels. In physiological solutions, 3.6% of the total current was carried by Ca^{2+}. The cation channels were not only permeable to Ca^{2+} but also to Mn^{2+}, as evidenced by the quench of Fura-2 fluorescence. Mn^{2+} current through 50-pS channels could not be resolved at the single-channel level. Our results suggest that 50-pS cation channels partially contribute to sustained increases of $[Ca^{2+}]_i$ in mast cells following receptor activation.**

In many nonexcitable cells, there appear to exist two main pathways for Ca^{2+} influx. One mechanism, also known as "capacitative" Ca^{2+} entry (1), is linked to the filling state of Ca^{2+} stores and upon depletion of cellular Ca^{2+} pools results in activation of a Ca^{2+}-selective current (2). The other mechanism is provided by nonspecific cation channels that may be classified as receptor- or second messenger-operated channels (3). Capacitative Ca^{2+} influx may also be activated independently of agonist stimulation by agents able to discharge the Ca^{2+} stores, such as inositol 1,4,5-trisphosphate ($InsP_3$), Ca^{2+} pump inhibitors, Ca^{2+} ionophores, or excess of Ca^{2+} chelators (2, 4). Mn^{2+} is often used as a tracer for calcium influx since Mn^{2+} quenches Fura-2 fluorescence without any interference due to intracellular calcium concentration ($[Ca^{2+}]_i$) changes, provided that the correct isosbestic point is selected (5, 6). Mn^{2+} dye-quenching experiments cannot unambiguously discern the pathways by which Mn^{2+} (and thus Ca^{2+}) enters the cytosol (7, 8). Using the patch-clamp technique, Lückhoff and Clapham (9) have shown that in endothelial cells extracellular ATP activates a Ca^{2+} and inositol 1,3,4,5-tetrakisphosphate-dependent current that admits Mn^{2+}.

Previous experiments have shown that in mast cells, influx of calcium occurs through two distinct pathways: nonspecific cation channels that are permeable to divalent cations (10–12) and a calcium-specific pathway that is activated by depletion of calcium from internal stores (2). The nonspecific channels are referred to as 50-pS channels, whereas the specific pathway has been given the name I_{CRAC} (for calcium release-activated calcium current). I_{CRAC} is a highly selective Ca^{2+} influx pathway that may be activated in parallel with 50-pS channels following agonist stimulation of mast cells. Here we report that intracellularly applied heparin prevents $InsP_3$-induced Ca^{2+} influx but does not interfere with agonist activation of 50-pS channels. This allows the relation between activity of 50-pS channels and $[Ca^{2+}]_i$ to be studied in isolation. Our results show that the cation channels activated by receptor stimulation are permeable to Ca^{2+} and Mn^{2+} but only partially contribute to the plateau phase of elevated $[Ca^{2+}]_i$ following the transient Ca^{2+} release from intracellular stores.

METHODS

Mast cells from rat peritoneum were obtained as described (13). For experiments, cells were transferred to the recording chamber and kept in a Ringer's solution of the following composition (in mM): NaCl 140, KCl 2.8, $CaCl_2$ 2, $MgCl_2$ 2, glucose 11, and Hepes-NaOH 10 (pH 7.2). External solution changes were made by pressure ejection (10 cmH_2O) from a wide-tipped puffer pipette positioned about 10–20 μm from the cell. The standard intracellular solution contained (in mM): potassium glutamate 145, NaCl 8, $MgCl_2$ 1, MgATP 0.5, Fura-2 pentapotassium salt (Molecular Probes) 0.1, and Hepes-KOH 10 (pH 7.2). $InsP_3$ (Amersham, 10 μM) or heparin (low molecular weight, Sigma, 500 μg/ml) was added when desired. Experiments were performed at room temperature (22–26°C) in the tight-seal whole-cell configuration of the patch-clamp technique using Sylgard-coated patch pipettes with resistances of 2–5 MΩ. Series resistances were in the range of 5–20 MΩ. Membrane currents were recorded as described (2). Variance analysis was used to identify the activation of 50-pS cation channels. This was performed on-line at a rate of 0.5–1 Hz by sampling 500-ms sections of membrane currents with a sampling rate of 5 kHz and low-pass filtered at 500 Hz (effective bandwidth: 2–500 Hz). Measurement of Fura-2 fluorescence from single mast cells in the whole-cell configuration was essentially as described (14). Experiments for estimating calcium fluxes through 50-pS channels and I_{CRAC} were performed by loading cells with a high concentration of Fura-2 (2 mM) according to the method described by Neher and Augustine (15). Leak currents were determined before activation of the respective influx pathways and used for leak correction of currents

The publication costs of this article were defrayed in part by page charge payment. This article must therefore be hereby marked "*advertisement*" in accordance with 18 U.S.C. §1734 solely to indicate this fact.

Abbreviations: $[Ca^{2+}]_i$, intracellular calcium concentration; $[Ca^{2+}]_o$, extracellular calcium concentration; $InsP_3$, inositol 1,4,5-trisphosphate; I_{CRAC}, calcium release-activated calcium current.

†Present address: Department of Biomedical Sciences, University of Padova, Via Trieste 75, 35131 Padova, Italy.

induced by square voltage pulses to negative membrane potentials (−100 mV). A ratio was defined between the absolute change in the calcium-sensitive fluorescence signal of Fura-2 (390 nm) and the leak-corrected current integral according to

$$R = \Delta F_{390} / \int Idt,$$

where R is the ratio, ΔF_{390} is the change in fluorescence at 390 nm, and $\int Idt$ is the current integral of I_{CRAC} or $I_{50\text{-pS}}$ measured during the voltage pulse.

RESULTS

Two Components of Ca^{2+} Influx in Rat Mast Cells. We have previously described the presence of two Ca^{2+} influx pathways in mast cells. One is carried by 50-pS cation channels (11) and the other is carried by a highly selective Ca^{2+} current (I_{CRAC}) that is controlled by the filling state of intracellular Ca^{2+} stores (2). Both pathways may be operating in parallel since agonists may activate cation channels through G proteins and Ca^{2+} release from intracellular stores through InsP_3 production.

When mast cells are challenged with secretagogues that induce inositol phospholipid breakdown, one usually observes a transient release of Ca^{2+} from intracellular stores followed by a sustained $[Ca^{2+}]_i$ increase that is due to Ca^{2+} influx (11). The amplitude and duration of this plateau phase of elevated $[Ca^{2+}]_i$ can be quite variable. Fig. 1*A* illustrates this variability by showing two typical responses induced by compound 48/80. Although the inward current in these cells was of the same magnitude, the plateau phase was quite different. We found more cells showing a low plateau phase

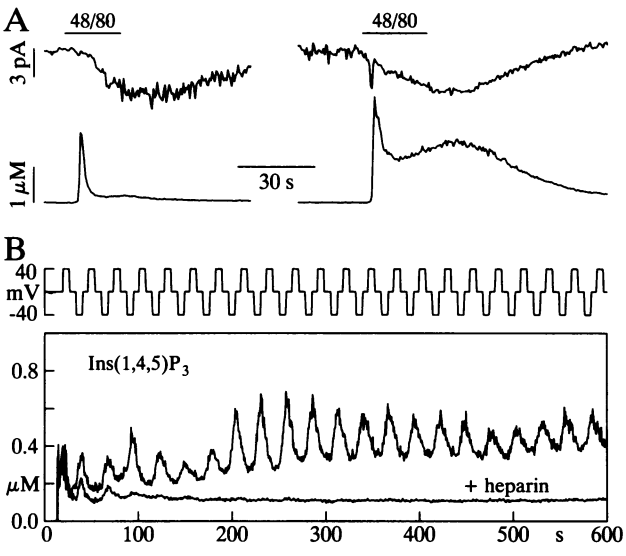

FIG. 1. Receptor- and InsP_3-mediated Ca^{2+} influx. (*A*) Examples of changes in $[Ca^{2+}]_i$ and membrane current induced by agonist stimulation with compound 48/80 (5 μg/ml). The upper traces show inward currents recorded at −40 mV in Ringer's solution extracellular calcium concentration {2 mM ($[Ca^{2+}]_o$)}. Note the similar amplitudes of inward current but the different amplitudes of $[Ca^{2+}]_i$ plateau (lower traces). (*B*) Effect of internally applied heparin on Ca^{2+} influx triggered by InsP_3. The upper trace shows the voltage protocol. The superimposed bottom traces show $[Ca^{2+}]_i$ calculated from Fura-2 fluorescence for two cells perfused with InsP_3 in the presence or absence of heparin. Hyperpolarization-driven Ca^{2+} influx accompanied each step to −40 mV in the cell without heparin, due to the activation by InsP_3 of the Ca^{2+}-influx pathway triggered by depletion of internal Ca^{2+} stores (I_{CRAC}). In the cell with heparin, Ca^{2+} influx occurred only initially and then rapidly died out.

(left panel) than a high plateau (right panel) (see also ref. 10). The difference between the resting $[Ca^{2+}]_i$ and the sustained $[Ca^{2+}]_i$ increase was 113 ± 24 nM (mean ± SEM, n = 13) and 1030 ± 189 nM (n = 7) for low and high plateaus, respectively. In the same experiments, however, no difference was noticed between the mean current amplitudes (−3.3 ± 0.6 pA for low plateaus and −3.4 ± 0.5 pA for high plateaus) and no correlation could be found between the peak Ca^{2+}-release transient and the sustained $[Ca^{2+}]_i$ increase.

To investigate the contribution of 50-pS channels to the sustained phase of elevated $[Ca^{2+}]_i$ it was necessary to prevent activation of I_{CRAC}. Heparin has been reported to inhibit InsP_3-dependent release of Ca^{2+} from internal stores by blocking the InsP_3 receptor (16). As shown in Fig. 1*B*, heparin also prevented the Ca^{2+} influx induced by InsP_3. The superimposed traces show $[Ca^{2+}]_i$ from mast cells dialyzed via patch pipettes containing InsP_3 without and with heparin. Without heparin, large hyperpolarization-driven increases in $[Ca^{2+}]_i$ were observed, as expected from InsP_3-dependent activation of the calcium-specific influx pathway (10). Similar results were observed in 14 of 18 mast cells dialyzed with InsP_3. With heparin, however, the pattern was different: only a few episodes of hyperpolarization-driven influx were observed following break-in, and the response died out with time, presumably as heparin diffused into the cell. In the presence of heparin, InsP_3-induced Ca^{2+} influx was blocked in 78% (18 of 23) of the cells.

Ca^{2+} Influx Correlates with Activity of 50-pS Channels. In 83% (139 of 167) of the cells, heparin abolished the large transient increase in $[Ca^{2+}]_i$ normally stimulated by compound 48/80, which has been shown to be caused by release of Ca^{2+} from InsP_3-sensitive stores (11). In mast cells perfused with heparin to prevent activation of calcium influx via I_{CRAC}, compound 48/80 activated an inward current at −40 mV (Fig. 2*A*). This potential was chosen to minimize contaminating chloride currents, which reverse at about −40 mV. This current represents activation of 50-pS channels, as verified by the variance increase, which is a fingerprint for activity of 50-pS channels in mast cells (11). In the absence of external Ca^{2+}, compound 48/80 produced no change in $[Ca^{2+}]_i$ in the heparin-treated cells; in the presence of external Ca^{2+}, an increase in $[Ca^{2+}]_i$ was correlated with the inward current, suggesting that the 50-pS channels conduct calcium (Fig. 2*A*).

In the examples shown in Fig. 2*A*, it is apparent that, although the change in $[Ca^{2+}]_i$ elicited by activation of 50-pS channels increased with increasing external calcium, the amount of current declined with increasing calcium. The overall relationship is summarized in Fig. 2*B*, where the peak change in $[Ca^{2+}]_i$ was plotted as a function of the peak current for a number of cells (n = 16–29) at three levels of $[Ca^{2+}]_o$. The slope of the linear regression was found to be 13 nM/pA of inward current at 2 mM $[Ca^{2+}]_o$, increasing to 34 nM/pA in 5 mM $[Ca^{2+}]_o$ and 96 nM/pA in 10 mM $[Ca^{2+}]_o$.

To establish the mechanism by which external calcium reduces current through 50-pS channels, the single-channel activity was observed in whole-cell recordings at different levels of $[Ca^{2+}]_o$. Because of the relatively large single-channel current through 50-pS channels compared to the chloride channels (10) and compared to I_{CRAC} (17), and because of the paucity of other ionic conductances in mast cells, individual openings of single 50-pS channels can be resolved in whole-cell recordings. To keep the overall level of activity low so that individual openings could be readily observed, spontaneous openings of 50-pS channels were recorded in unstimulated cells (10). We found that increasing external calcium from 2 mM to 10 mM affected the amplitude and the kinetics of 50-pS channel events, as illustrated in Fig. 3. The slope conductance declined from 42 pS in 2 mM $[Ca^{2+}]_o$ to 36 pS in 10 mM $[Ca^{2+}]_o$, in agreement with previous results showing that single-channel

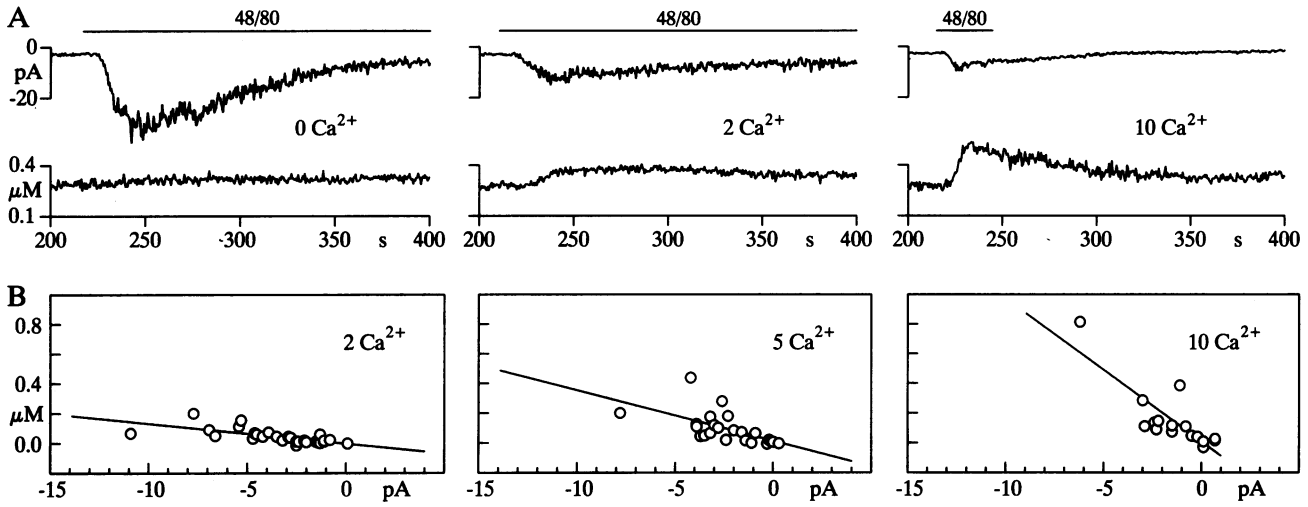

FIG. 2. Relation among current through 50-pS cation channels and $[Ca^{2+}]_i$. (*A*) Examples of membrane current (upper traces) activated by application of compound 48/80 (5 μg/ml) and the simultaneously determined $[Ca^{2+}]_i$ (lower traces) from three different mast cells at the indicated concentrations of external calcium. The duration of secretagogue application is indicated by the line above the traces. Heparin was present in the pipette solution in all three cells to suppress I_{CRAC}, and the holding potential in each case was −40 mV. The inward current elicited by compound 48/80 is due to activation of nonspecific cation channels (50-pS channels). (*B*) Summary of the relation between the peak change in $[Ca^{2+}]_i$ and the peak inward current elicited by compound 48/80. Each point represents the result from a single cell. The straight lines were fitted to the data by a least-squares criterion and had slopes of 13, 34, and 96 nM/pA of inward current for 2, 5, and 10 mM $[Ca^{2+}]_o$, respectively.

conductance was smaller in external solutions containing an elevated divalent cation concentration (11). In addition, the average open duration and the overall frequency of events were reduced in 10 mM $[Ca^{2+}]_o$, so that the fraction of time that one or more 50-pS channels were open (i.e., np_o, where n is the number of channels and p_o is the open probability for a single channel) declined from 0.097 ± 0.020 in 2 mM $[Ca^{2+}]_o$ to 0.061 ± 0.020 in 10 mM $[Ca^{2+}]_o$ (mean ± SEM, n = 5). Taken together, the effects of external calcium on channel conductance and np_o predict that the whole-cell current during agonist activation of 50-pS channels in 10 mM $[Ca^{2+}]_o$ should be about 50% of the current in 2 mM $[Ca^{2+}]_o$. This is in reasonable agreement with the mean whole-cell current measured during agonist activation (1.4 pA in 10 mM $[Ca^{2+}]_o$ vs. 3.4 pA in 2 mM $[Ca^{2+}]_o$, mean values derived from Fig. 2*B*).

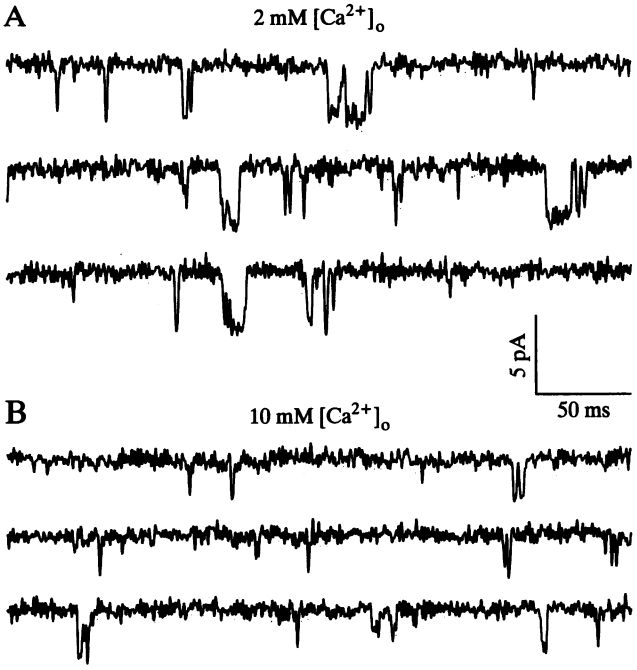

FIG. 3. Effect of external calcium on activity of 50-pS channels. Individual traces show samples of single channels observed during whole-cell recordings from an unstimulated mast cell bathed in 2 mM (upper traces) or 10 mM (lower traces) $[Ca^{2+}]_o$. Pipette potential was −60 mV. Traces were selected to show channel activity and are not representative of the overall frequency of channel opening. Recording bandwidth: 2–500 Hz.

Mn^{2+} Influx Through 50-pS Cation Channels. The quenching of Fura-2 fluorescence by Mn^{2+} has been widely used to study divalent cation influx. Because our results indicate that 50-pS channels are permeable to Ca^{2+}, we examined whether the channels would also pass Mn^{2+}, producing a quenching of Fura-2 fluorescence associated with channel activation. Fig. 4*A* illustrates that agonist stimulation in the presence of external Mn^{2+} (1 mM) caused a decrease in Fura-2 fluorescence at its isosbestic wavelength (360 nM), consistent with quenching by Mn^{2+} influx. The quenching of fluorescence followed the time course of the current through 50-pS channels, showing a slow recovery as the current inactivated. This suggests that Mn^{2+} influx occurred via 50-pS cation channels. We assessed the initial rate of fluorescence quenching by measuring the slope of Fura-2 fluorescence decrease (corrected for by the slope of the Fura-2 signal before application) while applying Mn^{2+} in the absence (control cells) or presence (stimulated cells) of 48/80. A basal Mn^{2+} quenching was always observed in unstimulated control cells (slope = −0.6 ± 0.1, arbitrary fluorescence units/s, mean ± SEM, n = 6). It may be accounted for by either spontaneous 50-pS activity or other Mn^{2+} entry pathways. During activation of 50-pS channels, the measured slope was −1.5 ± 0.2 (n = 7). This corresponds to a 2.5-fold average increase in the rate of fluorescence quenching in stimulated cells. We also attempted to look directly for Mn^{2+} current via 50-pS channels by examining the activity of single 50-pS channels in whole-cell recordings in the presence of Mn^{2+} as the only external cation. As shown in Fig. 4*B*, the spontaneous channel activity visible in Ringer's solution containing 2 mM Ca^{2+} disappeared in the presence of isotonic Mn^{2+} solution (115 mM $MnCl_2$).

Ca^{2+} Selectivity of 50-pS Channels. We compared the Ca^{2+} selectivity of 50-pS channels with that of I_{CRAC}, which we have previously found to be equivalent to that of voltage-activated calcium channels in chromaffin cells (17). This was achieved by using Fura-2 as the dominant intracellular buffer and recording both changes in the Ca^{2+}-sensitive fluores-

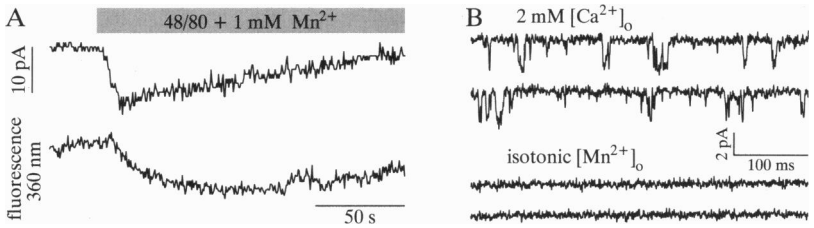

FIG. 4. Influx of Mn^{2+} via 50-pS channels. (*A*) Changes in membrane current (upper trace) and Fura-2 fluorescence (lower trace) in response to compound 48/80, applied in Ca^{2+}-free Ringer's solution containing 1 mM Mn^{2+} and 0.1 mM EGTA. The holding potential was −40 mV, and the pipette solution contained heparin. (*B*) Openings of 50-pS channels in whole-cell recordings before and during perfusion with isotonic Mn^{2+} (115 mM $MnCl_2$). The traces show samples of membrane current at a holding potential of −40 mV from an unstimulated mast cell bathed in 2 mM $[Ca^{2+}]_o$.

cence (390 nM) and whole-cell currents through 50-pS channels. Under these conditions, all incoming Ca^{2+} will bind to Fura-2 and together with the current integral this can be used to quantify the relative proportion of calcium that entered the cell during the current flow (15). Fig. 5 shows an example of a cell bathed in Ringer's solution containing 10 mM Ca^{2+} and intracellularly perfused with high Fura-2 (2 mM) and heparin. After loading was completed, 50-pS channels were activated by 48/80. Hyperpolarizing voltage pulses (−100 mV) were delivered before and after activation of the current to increase the driving force for calcium influx. The net inward current in response to these pulses was accompanied by a decrease in the Fura-2 fluorescence at 390 nm (see magnified inset). Similar experiments were carried out using InsP_3 or ionomycin to activate I_{CRAC} (data not shown, but see ref. 17). The ratio between the absolute amount of fluorescence reduction and the net charge transfer during the current flow (see *Methods*) was 15.6 ± 1.7 units·pA^{-1}·s^{-1} (mean ± SEM, n = 6) for 50-pS channels and 78.5 ± 20.3 units·pA^{-1}·s^{-1} (n = 3) for I_{CRAC}. Dividing these values gives a ratio of 0.20 of

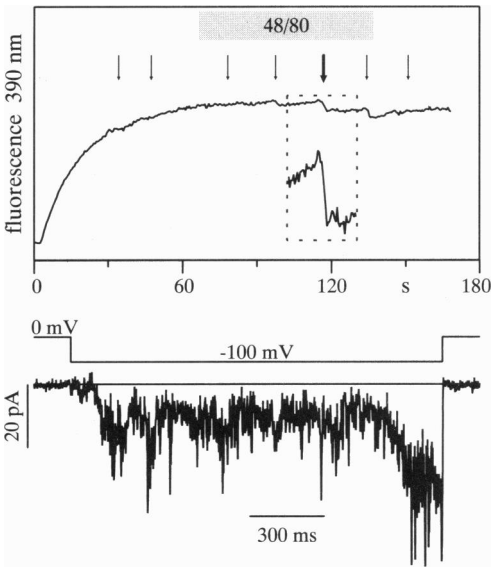

FIG. 5. Ca^{2+} selectivity of 50-pS channels. The Ca^{2+} selectivity of 50-pS channels was determined in comparison with that of I_{CRAC}. 50-pS channels were activated by 48/80, whereas concomitant activation of I_{CRAC} was prevented by intracellular perfusion with heparin. Changes in the Ca^{2+}-sensitive fluorescence at 390 nm and whole-cell currents were recorded in the presence of 2 mM Fura-2 as the dominant intracellular buffer (10 mM external Ca^{2+}). Inward currents were measured during hyperpolarizing voltage pulses to −100 mV (lower panel) delivered at the times indicated by the arrows. From the ratio between the fluorescence reduction (upper panel: thicker arrow and magnified inset) and the net charge transfer (lower panel), we estimated the relative Ca^{2+} selectivity of 50-pS channels compared to that of I_{CRAC} (see *Methods* and *Results*).

calcium current through 50-pS channels compared to I_{CRAC}. The same experiments, when carried out in 2 mM instead of 10 mM external Ca^{2+}, resulted in 2.9 ± 0.4 units·pA^{-1}·s^{-1} (n = 4) for 50-pS channels and 79.0 ± 10.1 units·pA^{-1}·s^{-1} (n = 5) for I_{CRAC}. This yields a relative ratio of 0.036 of calcium current through 50-pS channels compared to I_{CRAC}, under physiological conditions.

DISCUSSION

By analyzing the inward currents activated by agonist stimulation and the resulting changes in $[Ca^{2+}]_i$, we have determined the contribution of cation currents to receptor-mediated Ca^{2+} influx in mast cells. We discuss the relative Ca^{2+} permeability of a nonspecific cation channel and a highly selective Ca^{2+} influx pathway that is controlled by the filling state of intracellular Ca^{2+} stores (I_{CRAC}). The nonspecific cation channel was previously characterized as a 50-pS channel that is probably activated by G protein and inhibited by protein kinase C. Although its activation by secretagogues is often associated with Ca^{2+} mobilization from intracellular stores, the 50-pS channel is not directly activated by either Ca^{2+} or InsP_3 (11).

We employed heparin to prevent the InsP_3-induced Ca^{2+} influx through I_{CRAC} to study 50-pS channels in isolation. In the presence of heparin, activation of 50-pS channels induced a long-lasting Ca^{2+} increase dependent on $[Ca^{2+}]_o$. However, at higher external calcium, the current carried through 50-pS channels was effectively reduced. As previously suggested, high $[Ca^{2+}]_i$ may exert a negative feedback role (11). The present data suggest that increasing $[Ca^{2+}]_o$ affects the kinetics and the amplitude of 50-pS channels as is apparent from the decrease in the overall open probability accompanied by a minor reduction in the slope conductance. The reduction in the unitary conductance by Ca^{2+} ions permeating through cation channels has also been observed in cGMP-, nicotinic acetylcholine-, *N*-methyl-D-aspartate-, and ATP-gated channels (18–21). It seems to be a general feature of nonspecific cation channels and has been interpreted as a screening effect of divalent cations at the entrance of the channel (19). However, the reduction in the macroscopic current also appears to be influenced by the reduced open probability observed at higher Ca^{2+} concentrations. This contrasts with the recently described properties of the neuronal-type nicotinic channel, where, despite a reduced unitary conductance, an increase in the open probability accounts for an overall increase in the macroscopic current observed at higher external Ca^{2+} (22).

A large number of studies on Ca^{2+} influx has employed Mn^{2+} as a surrogate of Ca^{2+} by measuring Mn^{2+}-induced quenching of Fura-2 fluorescence. Our finding that the 48/80-induced cation current was paralleled by fluorescence quenching of Fura-2 suggests that 50-pS also admit Mn^{2+} ions. Although unitary currents were previously measured using isotonic $BaCl_2$ solution (10), similar recordings could

not be obtained with Mn^{2+}. This may be due to small, vanishing single-channel currents or to extremely short open times of the channels in isotonic $MnCl_2$ solution.

Although most of the inward current through 50-pS channels is carried by Na^+, the cation channels show a significant permeability to Ca^{2+} ions. The rather small current flowing through 50-pS channels and the relatively high contribution of the chloride current (10) at positive potentials prevent an accurate estimation of permeability ratios by reversal potential measurements. We used another approach to better quantify the Ca^{2+} permeability (15, 23) in which Fura-2 was used as the dominant intracellular Ca^{2+} buffer to report all incoming Ca^{2+} through 50-pS cation channels during a hyperpolarizing voltage step. The ratio between the change in the Ca^{2+}-sensitive fluorescence signal of Fura-2 and the current integral can be compared with the ratios, experimentally determined in a similar way, for I_{CRAC} and voltage-gated Ca^{2+} currents. Since I_{CRAC} has a Ca^{2+} selectivity equal to that of voltage-gated Ca^{2+} channels (17) and can therefore be considered as a "pure" Ca^{2+} current, one can estimate from the above-mentioned relationships the proportion of 50-pS current carried by Ca^{2+} ions. Under physiological conditions (i.e., 2 mM external Ca^{2+}) 3.6% of the current through 50-pS channels is carried by Ca^{2+}. This value increased to 20% in the presence of 10 mM external Ca^{2+}.

The constant-field current equation (Goldmann–Hodgkin–Katz current equation) can now be used to estimate the permeability ratio $P_{Ca^{2+}}/P_M$, where P_M is the permeability to Na^+ and K^+ ions (24). Starting from the Ca^{2+} permeability measured with the method described above and assuming Na^+ and K^+ ions to be equally permeant and Cl^- and Mg^{2+} ions to be impermeant, we obtained for the ratio $P_{Ca^{2+}}/P_M$ a value of 0.7 (2 mM external Ca^{2+}) and 1 (10 mM external Ca^{2+}). If one considers ionic activities instead of ionic concentrations, one arrives at slightly higher selectivity ratios, since the activity coefficient γ for Ca^{2+} is considerably smaller than for monovalents in solutions of physiological compositions [$\gamma = 0.27$ for Ca^{2+} and $\gamma = 0.77$ for Na^+ or K^+, as reported (19)]. This will increase the ratio $P_{Ca^{2+}}/P_M$ to 2.1 and 2.8 for 2 and 10 mM external Ca^{2+}, respectively. Among the nonspecific cation channels, the 50-pS channel shows a relatively high Ca^{2+} selectivity compared to the serotonin type 3 channel [$P_{Ca^{2+}}/P_{Na^+} = 0.55$ (25)], the muscle nicotinic acetylcholine channel [$P_{Ca^{2+}}/P_{Na^+} = 0.29$ (26)], and the α-amino-3-hydroxy-5-methyl-4-isoxazolepropionate/kainate channel [$P_{Ca^{2+}}/P_{Na^+} = 0.15$ (24)]. A similar or higher Ca^{2+} selectivity was reported for two other types of nonspecific cation channels: the ATP-gated channel described in smooth muscle cells [$P_{Ca^{2+}}/P_{Na^+} = 3.3$ (21)] and the *N*-methyl-D-aspartate-gated channel found in central neurons [$P_{Ca^{2+}}/P_{Na^+} = 10.6$ (24)]. One should, however, be cautious in comparing these data because different ionic conditions and activity coefficients were used.

Following agonist stimulation, a plateau phase of elevated $[Ca^{2+}]_i$ due to Ca^{2+} influx is observed in mast cells. As shown in Fig. 1*A*, in the absence of heparin, large differences in the size of the plateau were evident from cell to cell within a preparation or, more strikingly, across preparations. A possible explanation of this variability is that the small plateaus (seen in about 74% of the cells) represent influx due solely to 50-pS channels, whereas large plateaus are observed in cells in which the more potent Ca^{2+}-influx pathway, I_{CRAC}, is recruited. However, this does not seem to be the case; even the smaller plateaus, which average about 100 nM above resting $[Ca^{2+}]_i$, were larger than the increase of about 50 nM expected from the observed relation between $[Ca^{2+}]_i$ and current through 50-pS channels (3–4 pA of current; 13 nM/pA at 2 mM $[Ca^{2+}]_o$). This suggests that without heparin, I_{CRAC} contributes more than half of the plateau increase in $[Ca^{2+}]_i$ in cells with a small plateau phase. A different explanation is required, then, for the 20–30% of cells that show large plateaus (elevation of about 1 μM in $[Ca^{2+}]_i$); analysis of the amplitude of I_{CRAC} suggests that the large plateaus may occur in cells that have an unusually high density of I_{CRAC} (17). Thus, although the Ca^{2+} permeability of the 50-pS channels is significant, most of the incoming Ca^{2+} following agonist stimulation in intact mast cells is probably the result of activation of I_{CRAC}.

We thank M. Pilot for technical assistance. We acknowledge support from the following institutions: North Atlantic Treaty Organization (collaborative travel grant), European Molecular Biology Organization (long-term fellowship to C.F.), the Deutsche Forschungsgemeinschaft (Sonderforschungsbereich 236), and the Hermann- und Lilly-Schilling-Stiftung.

1. Putney, J. W. (1990) *Cell Calcium* **11**, 611–624.
2. Hoth, M. & Penner, R. (1992) *Nature (London)* **355**, 353–356.
3. Tsien, R. W. & Tsien, R. Y. (1990) *Annu. Rev. Cell. Biol.* **6**, 715–760.
4. Mason, M. J., Garcia-Rodriguez, C. & Grinstein, S. (1991) *J. Biol. Chem.* **266**, 20856–20862.
5. Sage, S. O., Merritt, J. E., Hallam, T. J. & Rink, T. J. (1989) *Biochem. J.* **258**, 923–926.
6. Jacob, R. (1990) *J. Physiol. (London)* **421**, 55–77.
7. Meldolesi, J., Clementi, E., Fasolato, C., Zacchetti, D. & Pozzan, T. (1991) *Trends Pharmacol. Sci.* **12**, 289–292.
8. Kass, G. E. N., Llopis, J., Chow, S. C., Duddy, S. K. & Orrenius, S. (1990) *J. Biol. Chem.* **265**, 17486–17492.
9. Lückhoff, A. & Clapham, D. (1992) *Nature (London)* **355**, 356–358.
10. Penner, R., Matthews, G. & Neher, E. (1988) *Nature (London)* **334**, 499–504.
11. Matthews, G., Neher, E. & Penner, R. (1989) *J. Physiol. (London)* **418**, 105–130.
12. Kuno, M. & Kimura, M. (1992) *J. Membr. Biol.* **128**, 53–61.
13. von zur Mühlen, F., Eckstein, F. & Penner, R. (1991) *Proc. Natl. Acad. Sci. USA* **88**, 926–930.
14. Neher, E. (1989) in *Neuromuscular Junction*, eds. Sellin, L. C., Libelius, R. & Thesleff, S. (Elsevier, Amsterdam), pp. 65–76.
15. Neher, E. & Augustine, G. J. (1992) *J. Physiol. (London)* **450**, 273–301.
16. Cullen, P. J., Comerford, J. G. & Dawson, A. P. (1988) *FEBS Lett.* **228**, 57–59.
17. Hoth, M. & Penner, R. (1993) *J. Physiol. (London)*, in press.
18. Matthews, G. (1991) *Trends Pharmacol. Sci.* **12**, 245–247.
19. Decker, E. R. & Dani, J. A. (1990) *J. Neurosci.* **10**, 3413–3420.
20. Ascher, P. & Nowak, L. (1988) *J. Physiol.* **399**, 247–266.
21. Benham, C. D. & Tsien, R. W. (1987) *Nature (London)* **328**, 275–278.
22. Mulle, C., Lena, C. & Changeaux, J. P. (1992) *Neuron* **8**, 937–945.
23. Schneggenburger, R., Zhou, Z., Konnerth, A. & Neher, E. (1993) *Biophys. J. Abstr.* **64**, 17326.
24. Mayer, M. L. & Westbrook, G. (1987) *J. Physiol. (London)* **394**, 501–527.
25. Young, G., Mathie, A. & Hille, B. (1992) *J. Physiol. (London)* **448**, 237–256.
26. Adams, D. J., Dwyer, T. M. & Hille, B. (1980) *J. Gen. Physiol.* **75**, 493–510.